The High Temperature Creep Behavior of Doped Tungsten Wire

P. K. WRIGHT

The creep behavior of 0.018 cm diam doped tungsten wire has been studied over a range of stress from 30 to 90 MPa and temperature from 2400 to 2800 K. Grain aspect ratio (gar) had a strong influence on creep and rupture of the recrystallized wires, and separated the creep behavior into two regimes with a transitional gar of about 11 between the two. The low gar regime showed lower strength and characteristics typical of grain boundary sliding. In the high gar regime, properties were independent of gar, and evidence is presented to show that creep is governed by dislocation-bubble dispersion strengthening.

DOPED tungsten wire is the preferred material for a wide range of incandescent lamp filaments, because of its excellent resistance to creep deformation at the highly elevated temperatures at which most lamps operate (2000 to 3200 K). Despite the exceptional characteristics of this material and its long history of usage (since 1921) only recently has much attention been devoted to characterizing and understanding the nature of its elevated temperature deformation.

It has long been understood that the creep resistance of doped tungsten is related to the highly elongated and overlapping grain structure developed upon recrystallization* of the wire filaments. Recently, much work[1-4] has been conducted in demonstrating the important role that potassium containing bubbles, formed from potassium introduced in the doping process, play in the development of the grain structure. Previous studies of creep in recrystallized doped tungsten by Moon and Stickler[5] on coils and Pugh[6] on straight wire demonstrated a marked decrease in creep rate compared to undoped material. Activation energies of 540 kJ (130 kcal) and stress exponents of 8.4 to 25 were found. The strengthening was interpreted as being partly a result of the larger grain size of the doped wire and partly due to dispersion strengthening by the potassium dope bubbles.

Although both previous studies recognized the importance of elongated grain structure, no attempt was made to quantify its effects on creep. In the light of recent work in thoriated nickel-base alloys[7,8] which clearly demonstrates the dependence of high temperature creep in dispersion strengthened systems on grain aspect ratio, it is important that the effect of this parameter on creep and rupture of doped tungsten wire be determined. This then allows a consideration not only of the importance of grain boundary deformation, but of the nature and magnitude of bulk grain deformation as well. As a consequence, this paper examines the high strength and remarkable creep characteristics of doped tungsten wire in the light of dispersion strengthening theories.

*The formation of the overlapping grain structure will be termed throughout this paper as "recrystallization," although the exact nature of the process is one of secondary or exaggerated grain growth rather than primary recrystallization.[1,2]

APPARATUS AND PROCEDURE

Creep testing was performed by hanging weights on a 20 cm vertical gage length of wire and heating by self resistance. Electrical contact was made at the top support and at the bottom of the wire through a flexible braided copper lead which did not interfere with the elongation of the wire. Wire temperatures were determined initially by optical pyrometry, but excellent control of temperature (±10 K) could be maintained by control of wire voltage and current once the voltage and current parameters as a function of temperature had been determined for a given wire size and gage length.

The upper end of the 20 cm gage length of wire was supported by water cooled glass tubing in order to minimize errors in creep rate due to thermal expansion of the support. Elongation of the wire was measured with an LVDT, the core being attached to the bottom of the loading system on the wire. All creep testing was performed in vacuum at pressures below 7×10^{-5} Pa (5×10^{-7} Torr).

Wires were tested in one of two ways:

A) Prior to insertion into the creep apparatus, the wires were recrystallized by heating to 2800 K at a predetermined rate and holding for 10 minutes. The rate most commonly used was switching on to full power ("flashing") at approximately 2000 K/s, although slower rates were occasionally used, as noted.

B) As-drawn wires were mounted in the apparatus, loaded and "flashed" to test temperature to begin testing.

MATERIALS

Four different doped tungsten (GE type 218) wires, approximately 183 μm in diam were studied. These wires, designated 1 through 4, were chosen to represent a wide range of recrystallized microstructure, as shown in Fig. 1. Because of the very long grain sizes obtained in these wires, it is difficult to represent the microstructures adequately in short sections. Grain aspect ratio (average grain length divided by average grain width) for these wires was measured on 2.0 cm sections of wire which had been recrystal-

P. K. WRIGHT, formerly with the Lamp Business Division of General Electric Company, E. Cleveland, Ohio, is now with the Aircraft Engine Group, General Electric Company, Evendale, OH 45215.

M Manuscript submitted March 21, 1977.

ISSN 0360-2133/78/0710-0955$00.75/0

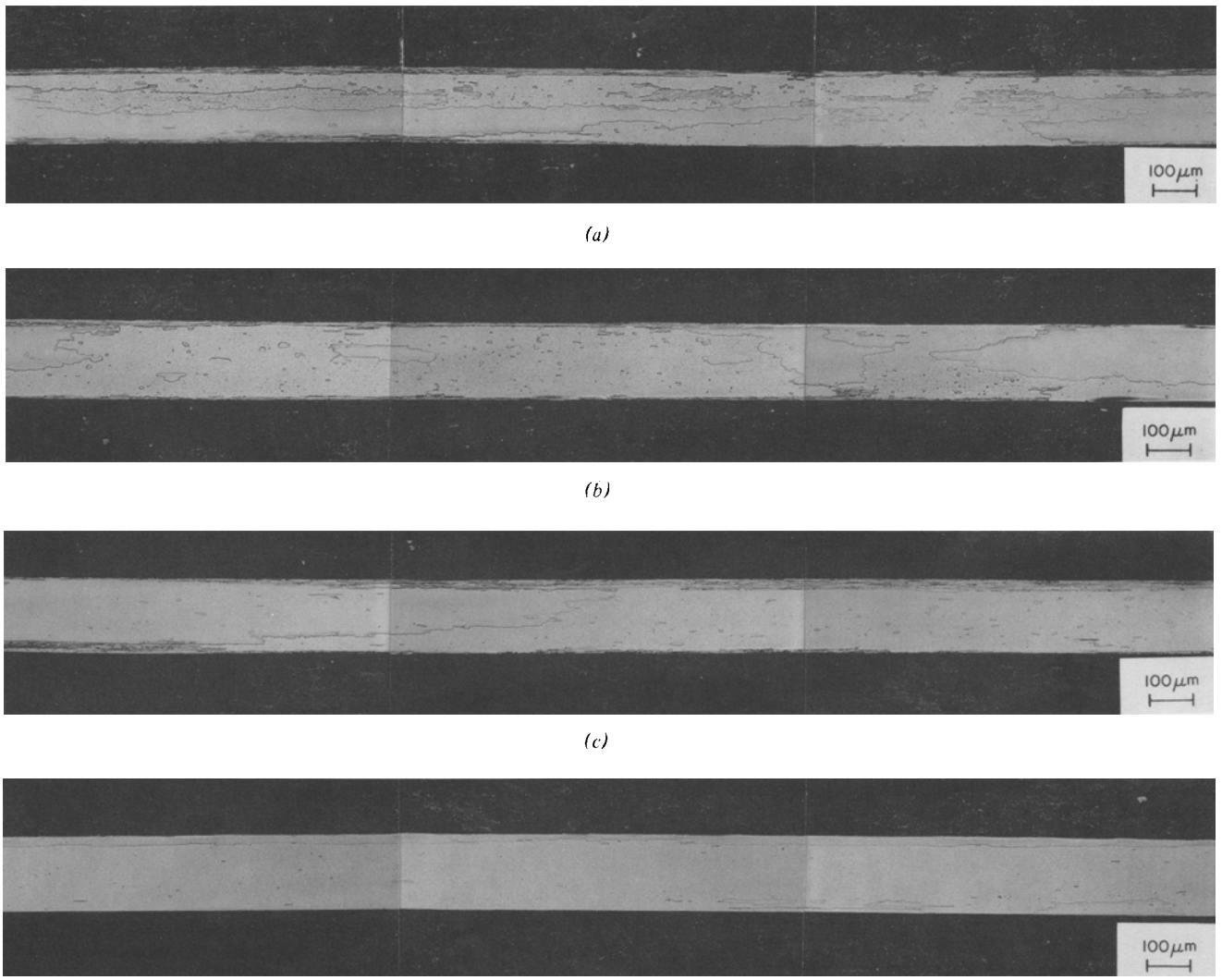

Fig. 1—Microstructures of 0.0183 cm diam doped tungsten wire after recrystallization by "flashing" (2000 K/s) to 2800 K and holding for 10 min, (*a*) Wire 1, (*b*) Wire 2, (*c*) Wire 3, and (*d*) Wire 4.

lized and creep tested. These aspect ratios are reported in Table I. It can be seen that when flashed (2000 K/s) wire 2 had the smallest aspect ratio and wire 4 had the largest. Except for wire 2, almost all grains occupied the entire width of the wire. These wires had varying sensitivity of final structure to heat up rate during recrystallization. A relatively slow rate of heat up (4.3 K/s) produced the grain aspect ratios listed in Table I. The wire to wire differences in grain aspect ratios were considerably less with this treatment, with most wires showing a substantial increase in grain aspect ratio, compared to "flashing."

Wires 1, 2, and 3 were analyzed for bulk potassium content and all three were found to contain 68 ± 3 ppm potassium by weight.

RESULTS

Creep curves were generated for wires 1, 2, and 3 as a function of temperature at a constant stress (in the range of 70 to 80 MPa) and for wires 2, 3, and 4 as a function of stress at 2800 K. While not all of the wires were recrystallized at the start of the test (as in treatment B, above), recrystallization proceeded rather rapidly at the test temperatures, so that the minimum creep rates observed represent creep in a recrystallized structure.

Typical creep curves are shown in Fig. 2. Creep rates were quite low, less than 2×10^{-6} s^{-1}, even at the highest stresses studied. Creep was relatively constant over the largest time portion of the test, and primary creep was quite small in material recrystallized prior to loading. Wires initially unrecrystallized showed a short lived but large primary creep regime. Tertiary creep at the end of a test was very brief and small in extent, being practically negligible. Total elongation at rupture was typically very small,

Table I. Effect of Recrystallization Rate on Grain Aspect Ratio and Creep-Rupture Properties at 2800 K and 75 MPa

	Flashed		10 min Rise	
Wire	gar	t_r, min	gar	t_r, min
1	19 ± 8	100	65 ± 20	423
2	4 ± 0.5	18	45 ± 20	764
3	35 ± 10	180	35 ± 10	100
4	60 ± 20	150	65 ± 20	334

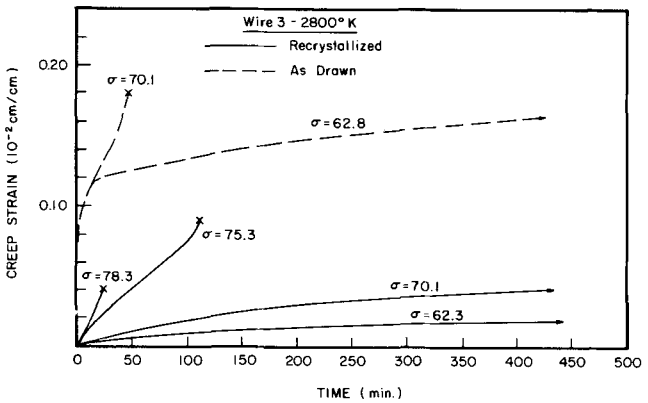

Fig. 2—Typical creep curves of doped tungsten wires at 2800 K: Wire 3 with heat treatments A and B. Stress in MPa.

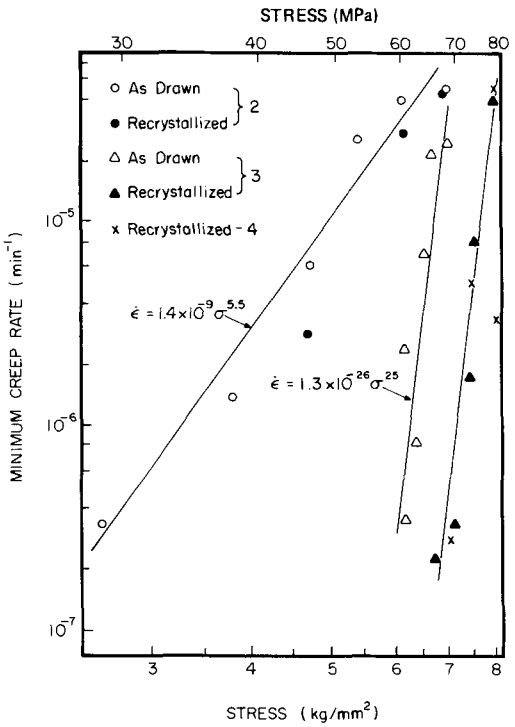

Fig. 3—Stress dependence of creep rate at 2800 K for doped tungsten wires. Note various heat treatments.

0.2 pct or less, similar to the values obtained by Horascek,[9] and decreased slightly with decreasing stress.

Dependence of Creep and Rupture on Stress and Temperature

At 2800 K, the stress dependence of minimum (steady-stage) creep rate in "flashed" material varied markedly depending on the wire tested. This is shown in Fig. 3, where minimum creep rate is plotted against the logarithm of stress. For the range of data observed, a conventional power-law equation was found to adequately describe the data. The stress exponent, n, varied from 5.5 for wire 2 to 25 for wires 3 and 4, for both test procedures A and B (recrystallized by "flashing" before or during the test). The rupture times of these materials showed similar dependence on stress, as shown in Fig. 4, with the stress exponent varying from 9.3 for wire 2 to 16.5 for wires 1, 3, and 4.

The temperature dependence of minimum creep rate is shown in Fig. 5, for samples unrecrystallized prior to testing (treatment B). The data displayed represent specimens which were completely recrystallized relatively early in the test so that the minimum creep rates are all for recrystallized material. The apparent activation energies based on minimum creep rates can be determined from the data shown in Fig. 5 to be about 620 kJ (150 kcal) for wire 2 and about 1600 kJ (380 kcal) for wires 1 and 3. These levels of temperature dependence were also reflected in the stress rupture behavior, with the activation energies for failure time being 390, 610, 650, and 1500 kJ for wires 2, 3, 4, and 1, respectively.

A comparison of the steady state creep rates obtained here at 2800 K agrees well with data previously obtained by Pugh[6] and Moon and Stickler[5] at slightly different temperatures, the present data representing a lower stress extension of the earlier results.

While most of the results reported are for material initially as drawn (treatment B), a significant number of tests were performed on samples recrystallized by "flashing" before testing (treatment A). Besides the difference in the primary creep behavior mentioned above, an enhancement in rupture strength was seen

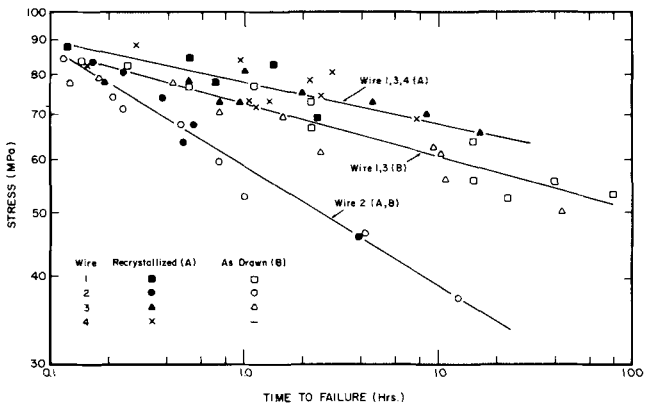

Fig. 4—Stress dependence of time to failure for doped tungsten wires at 2800 K. Both heat treatments A and B displayed.

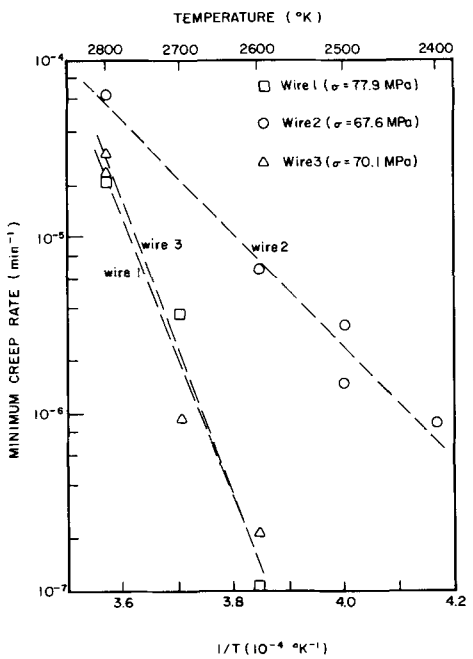

Fig. 5—Temperature dependence of creep rate (stress as noted) for doped tungsten wires. Treatment B.

in all wires with the exception of wire 2 (Fig. 4). Wire 3 also showed a change in creep rate (Fig. 3). In all cases, the stress and temperature dependencies of creep were identical for both treatments.

The degradation of creep rupture properties in samples initially in the as-drawn condition was probably due to creep damage that occurred early in the test while the wire was undergoing recrystallization. The fine grained as-drawn structure has poor creep resistance due to the proliferation of grain boundary sliding and cavitation. Void formation occurring prior to recrystallization would accelerate failure after recrystallization.

Effect of Grain Aspect Ratio

The microstructure of this material is somewhat different than for other materials in which grain aspect ratio correlations have been studied in that most of the grains extend entirely across the cross sections of the wire. Thus, the gar reported represent grain length divided by grain width dimensions and not necessarily the actual length of grain boundary overlap from one grain to another. Observation of the microstructures shows the two features to be correlated, so that gar, as reported, remains a valid parameter.

The dependence of rupture time on grain aspect ratio is clearly shown in Fig. 6, where the rate of recrystallization (prior to testing) was varied to produce a range of grain aspect ratios. It is seen that time to failure under constant conditions increases rapidly with increasing grain aspect ratio up to a gar of about 11. Above this critical aspect ratio, no further increase in rupture time occurs with further increases in gar. Wires 1, 3, and 4 lie above this critical gar for all recrystallization treatments, so their creep-rupture properties, as observed, are independent of recrystallization rate or grain length. Wire 2, however, has a relatively fine grain size when flashed, and thus has less than the critical aspect ratio for creep. When the grain size of wire 2 is increased by slower recrystallization rates to aspect ratio greater than 11, its rupture properties become similar to the other wires (Table I).

A similar behavior was observed in the steady state creep rates obtained, with identical creep rates observed in wires 1, 3, and 4 (Fig. 3) although the recrystallized gar of the wires ranged from 20 to 60 (Table I). Wire 2, with gar = 4, showed much more rapid creep rates and sensitivity to gar. The critical gar for creep also appears to be about 11.

Transmission Electron Microscopy

A few creep-rupture tested wires were examined by transmission electron microscopy by vapor depositing tungsten on the samples to facilitate handling, and then thinning to foils.[10] The photomicrographs (Figs. 7 and 8) show the characteristic rows of bubbles distributed along the wire drawing direction. In many areas of the wire, these were the only structural features. Near the surface of some of the wires, particularly wire 3, relatively fine grains were retained, in many cases pinned by bubble rows. Isolated grains within the wire interior (Fig. 7) were also seen in all the wires. Dislocation density varied widely from place to place in a given foil, as illustrated in Fig. 8, but was generally quite low. In all cases dislocations appeared strongly attracted to bubbles. Occasionally, regular networks appeared, as in Fig. 7, both in creep tested and in as-recrystallized material, thus indicating that these subgrain boundaries are remnants of structures existing prior to the exaggerated grain growth rather than creep subgrains.

Characterization of the bubble dispersion was obtained from photomicrographs of the foils. Three dif-

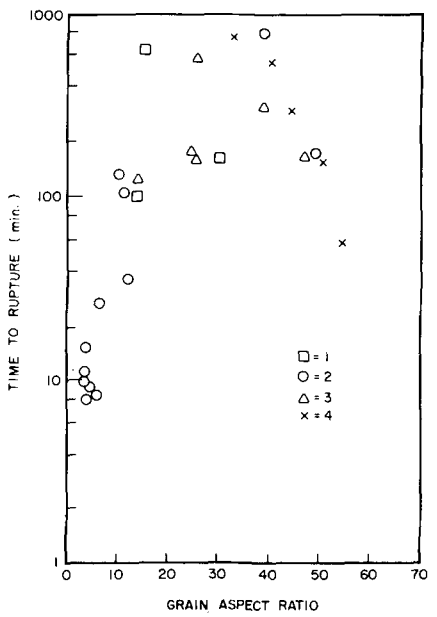

Fig. 6—Dependence of time to rupture at 2800 K and 73.6 MPa on grain aspect ratio for various doped tungsten wires.

Fig. 7—TEM photomicrograph of wire 3 creep tested by flashing under load (Treatment B) at 2650 K. Test time was 50 min.

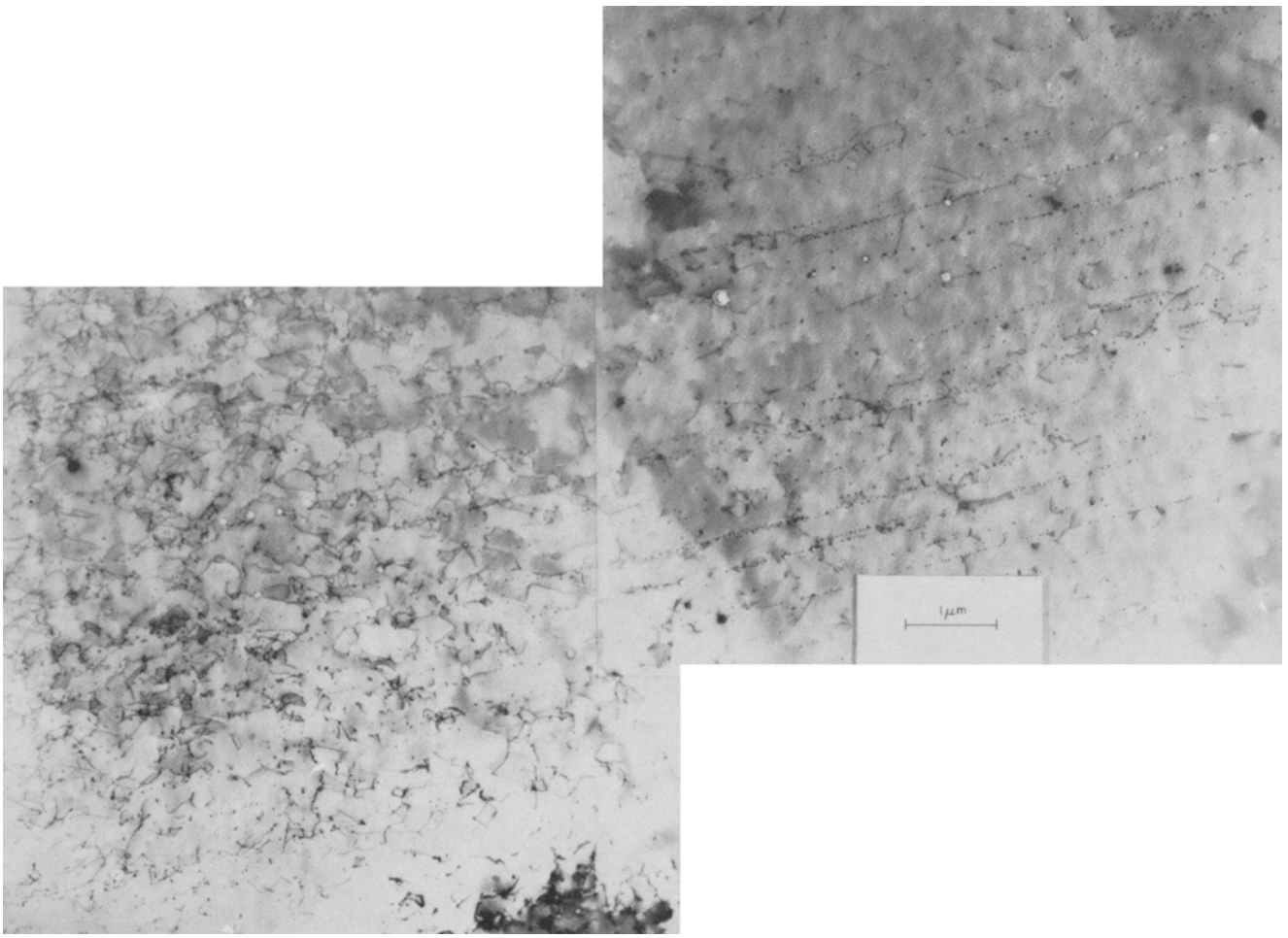

Fig. 8—TEM photomicrograph of wire 2, recrystallized by heating to 2800 K at 4.3 K/s, prior to creep testing. Crept at 2800 K for 30 min. (Photo courtesy of D. B. Snow.)

ferent areas from different foils were analyzed, approximately 10 to 20 μm^2 of foil area per wire being surveyed. No attempt was made to account for the possibility of some bubbles being rendered invisible by diffraction contrast conditions.[13] While there was some foil-to-foil variation, as shown in Table II, these differences were not significant. As shown in Table II, the mean bubble diam in all of this material was about 9 nm.

From the observed bubble size distributions, the volume fraction of bubbles was estimated by assuming a foil thickness of 0.1 μm. This calculation showed that the volume fraction of bubbles was of the order of 0.2 to 0.3 pct (Table II). The resulting nearest neighbor bubble-to-bubble spacing, Δ,[16] shown in Table II was obtained from the volume fraction, V_f, and mean bubble radius, a:

$$\Delta = 1.2\, a \left(\frac{2\pi}{3V_f} \right)^{1/2}.$$

While this relationship is strictly valid only for a random dispersion, and many of the bubbles are clearly in rows, it is doubtful whether any more accurate estimate is warranted in view of the approximations already involved in the dispersion characterization.

Table II. Bubble Dispersion Characteristics for Doped Tungsten Wires 1 and 2

		Average Bubble Diam, nm	Volume Fraction Bubbles	Average Nearest Neighbor Spacing, nm
Wire 1	Foil A	8.2	0.0018	450
	Foil B	9.0	0.0022	480
	Foil C	10.0	0.0012	750
	Overall	9.0	0.0017	560
Wire 2	Foil A	8.7	0.0029	390
	Foil B	8.0	0.0039	420
	Foil C	11.3	0.0031	500
	Overall	9.4	0.0033	440

Fracture Mode

Observations of fracture surfaces of the wires by scanning electron microscopy revealed two types of fracture surfaces, in general agreement with the observation of Pugh.[6] At relatively high stresses and short failure times, chisel-type fractures were observed in wires 1, 3, and 4 (Fig. 9), while at lower stresses in 1, 3, and 4, and at all stresses in wire 2, intergranular separation occurred (Fig. 10). Despite the change in fracture appearance with stress in wires 1, 3, and 4, there was no detectable change in failure kinetics (stress and temperature dependence) associated with the different modes.

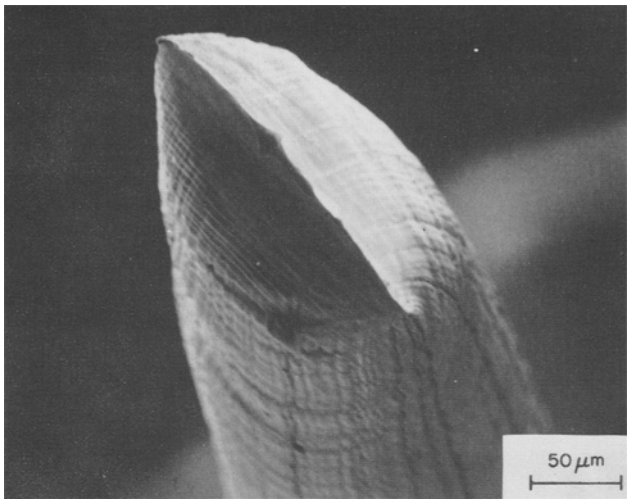

Fig. 9—Chisel-type slip fracture observed in high stress tests of high gar doped tungsten.

Fig. 10—Grain boundary failure observed in low gar material.

DISCUSSION

From the results presented above, it is clear that there are two principal types of creep behavior in doped tungsten wire, depending on the grain morphology as measured by grain aspect ratio. At relatively low gar, below a value of 11 for this material, creep rates are relatively high and failure times short. The moderate stress dependence (n = 5) and apparent activation energy near that of volume self diffusion for tungsten[17] (630 kJ/mole) suggest a diffusionally controlled process for this regime. The universal occurrence of fracture at grain boundaries and the strong dependence of creep and failure time in this regime on grain aspect ratio indicate that grain boundary sliding is an important deformation mechanism here. However, the creep resistance of even the smallest aspect ratio material (gar ~ 4) is far superior to any undoped material.[6,22] This may be due in part to the greater diffusional distances involved in accommodating sliding in the large, irregularly shaped doped tungsten grains. It is also quite likely, however, that deformation within the grains must be induced to some extent to accommodate sliding, so that a part of the strength increment of fine grained doped tungsten is due to contributions from the bulk strengthening mechanisms discussed below.

Above the critical grain aspect ratio the creep characteristics are quite unique, and a considerable amount of evidence will be presented to show that, in this regime, dispersion strengthening through dislocation-dope bubble interactions controls the creep properties of doped tungsten. Because creep of the wire in this regime is grain aspect ratio independent, contributions from grain boundary sliding are ruled out. Evidently, as suggested previously,[5,7] the degree of grain boundary overlapping is so great above an aspect ratio of 11, that the shear stress on the boundaries has been reduced to the point where grain boundary sliding proceeds at a slower rate than deformation within the grains. This type of grain aspect ratio dependence of strength has been seen in several other dispersion strengthened systems as well.[7,8,18] The fracture surface appearances for high gar materials at high stresses reinforces the idea that bulk grain deformation controls creep and failure, since chisel-type slip fractures are common under these conditions (Fig. 9).

An additional experiment was performed to demonstrate that the high creep resistance of doped tungsten is not solely due to the suppression of grain boundary sliding by high aspect ratio grains. A few samples of undoped tungsten were obtained that had been zone recrystallized to produce high grain aspect ratio structures (Fig. 11). These samples were kindly supplied by the Refractory Metals Laboratory of General Electric Company, Lamp Business Division. Stress rupture testing of these samples at 2800 K showed (Fig. 12) that their short time strengths were identical to equiaxed grained undoped material produced by nondirectional recrystallization (Fig. 11). Thus, even the relatively low grain aspect ratio doped material (wire 2) showed a considerable strength increment over even very high aspect ratio undoped material. This is in agreement with the tensile strength measurements by Pugh,[6] which showed a 55 MPa strength increase of doped over undoped tungsten at 2800 K.

The high apparent activation energies and volumes observed in high gar material are typical of other dispersion strengthened systems[7,8,18-21] and cast doubt as to whether creep is controlled solely by a diffusional mechanism, since any such process would inherently have the relatively low stress and temperature dependence typical of diffusional processes in tungsten ($n \leq 7$, $Q \leq 630$ kJ/mole).[17] Thus, the mechanism of creep by vacancy diffusion interaction with bubbles as proposed by Horascek[9] seems unlikely. The invocation of a large internal stress due to dislocation structure (necessary to reduce high apparent activation energies to more typical values) seems

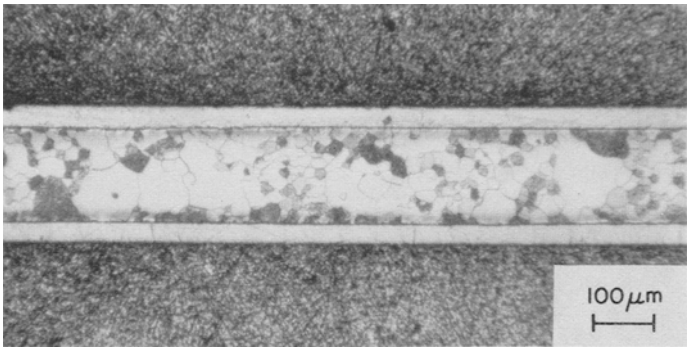

(a)

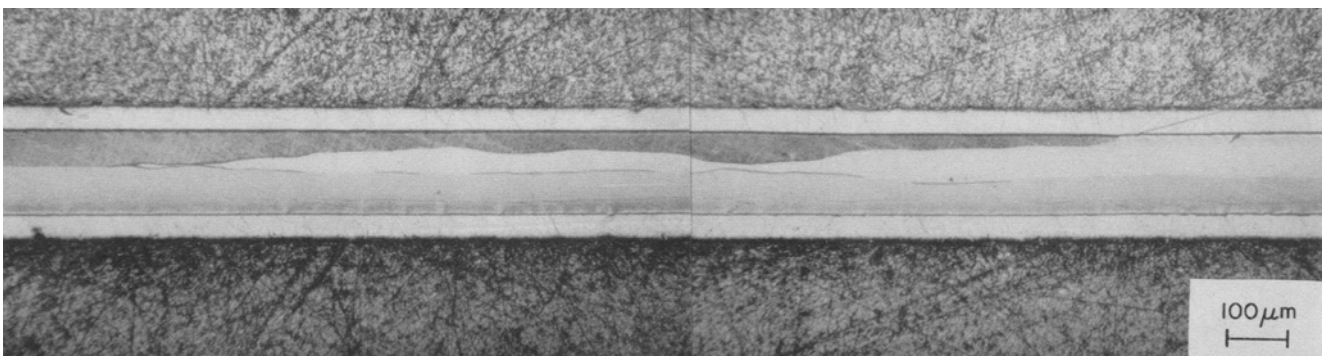

(b)

Fig. 11—Microstructures of undoped tungsten wires rupture tested at 2800 K. Nickel plated layer surrounds each wire. *a*) "flashed" to 2800 K, held 10 min. *b*) zone recrystallized prior to testing at 2800 K.

inappropriate here since the material is fully recrystallized and the dislocation density is quite low as seen in the electron micrographs. One common high temperature creep mechanism, climb of dislocations over obstacles, seem particularly unlikely, since the dislocations will be highly attracted to, and tightly bound by, the bubble obstacles due to elastic interactions. Climb-bowing also would be restricted due to the nature of the restraint on the dislocation at the bubble.

The overwhelming body of evidence, then, suggests that creep and rupture in structures above the critical grain aspect ratio is controlled by a potent bulk (rather than grain boundary) strengthening mechanism, similar in character to other dispersion strengthened systems. It is possible to examine this in more detail to ascertain its validity and nature.

In dispersion strengthened systems, slip is controlled generally either by obstacle cutting or Orowan bowing, depending on the obstacle strength. Bubble obstacle strength arises from two factors: 1) Elastic interaction between dislocation and bubble, and 2) Generation of new surface area by the passage of dislocations. Weeks, *et al*[22] have determined the elastic interaction energy of a screw dislocation and a spherical bubble of radius a, lying symmetrically on the dislocation as:

$$E_{\text{elastic}} = \frac{-Gb^2a}{2\pi}\left(\frac{\pi^2}{12} + \ln\frac{a}{r_o}\right). \qquad [1]$$

Using a core radius r_o of $2b = 5.0 \times 10^{-10}$ m, an average bubble radius, a, of 5.0×10^{-9} m, and the shear modulus of tungsten, G, at 2800 K of approximately 10^{11} N/m^2,[17,23] the interaction energy, E_{elastic}, is 2.0×10^{-17} J. This is a rather sizeable interaction energy, and it is not surprising, therefore, to observe in the electron micrographs that nearly all dislocations are pinned to bubbles.

The energy required to generate new surfaces in the bubble caused by the relative displacement of the two halves of the bubble after dislocation passage is:

$$E_{\text{surface}} = -2\gamma ab. \qquad [2]$$

Using the literature values of surface energy, $\gamma = 2.7$ J

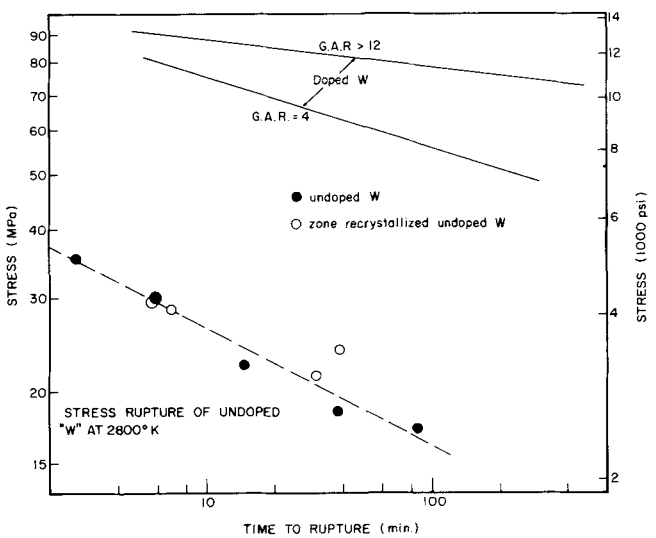

Fig. 12—Stress dependence of rupture at 2800 K for doped and undoped tungsten wires.

(Ref. 24, 25) and the same bubble radius and Burgers vector, the surface energy term is: $E_{surface} = 0.8 \times 10^{-17}$ J. Thus, the total obstacle energy is about 2.8×10^{-17} J. The flow stress increment due to this strength obstacle can be estimated, following Weeks, *et al*,[22] by assuming that the derivative of the interaction energy with respect to the distance of the dislocation from the bubble is approximately E/a, that is, most of the interaction energy arises within one radius of the bubble. Then

$$F_{max} = \tau bL = -E/a$$

where L is the interbubble nearest neighbor spacing, taken here from the electron micrographs as $L \simeq 500 \times 10^{-9}$ m (Table II). The flow stress increment τ_c due to bubble cutting then is:

$$\tau_c = 39 \times 10^6 \text{ N/m}^2 \text{ (39 MPa)}. \quad [3]$$

If the strength of the crystal is governed by Orowan bypass rather than by obstacle cutting, the Orowan equation should apply.[26,27]

$$\tau_B = \frac{Gb}{2\pi L} \ln\left(\frac{R}{r_o}\right) \quad [4]$$

where all quantities are as defined above. Setting $R = a$, (rather than the more customary $L/2$, which applies to an isolated loop) accounts for interactions with the dislocation loop on the other side of the obstacle.[27] Then:

$$\tau_B = 23 \times 10^6 \text{ N/m}^2 \text{ (23 MPa)}. \quad [5]$$

It is significant that these two estimates of the strength increment due to bubble-dislocation interactions agree quite well with the difference in strength between doped and undoped materials observed at short times (Fig. 12). For instance, the one minute tensile rupture strength of undoped tungsten at 2800 K is about 43 MPa, while that of doped tungsten (above critical gar) is about 100 MPa, a difference of 57 MPa. This converts to a shear strength increment of 28 MPa ($\sim \sigma/2$), close to the increments calculated by Eqs. 3 and 5. This lends considerable validity to the proposition that dislocation-bubble interaction strengthening is operating in doped tungsten, an idea suggested also by Moon and Stickler[5] and Pugh.[6]

Since the short-term strength of high grain aspect ratio doped tungsten appears to be satisfactorily described by direct dislocation-bubble strengthening, and since the long-term creep behavior is an excellent extrapolation of short term behavior, it appears that the high creep strength, and high activation energy and volume of creep are due also to the same mechanism. Unfortunately, the theoretical treatment of this subject is somewhat lacking. Coulomb[28] and Guyot[29] have developed models for the thermally activated bypass of voids (Coulomb) and hard particles (Guyot) by dislocation bowing. These models do indeed predict extremely high activation energies and volumes for such a process. Coulomb[28] finds an activation energy of

$$\Delta H = \mu b^3 \frac{a}{b}\left(1 - \frac{\sigma}{\mu}\frac{L}{b}\right) \quad [6]$$

for a dislocation being activated over a row of three bubbles. Inserting the appropriate parameters for these doped tungsten materials, one finds an activation energy of 2.2×10^6 J, at a stress of 0.9 of the Orowan stress; that is, at about 92 MPa. This value is approximately twice that observed (1.25×10^6 J), and increases steeply with decreasing stress. The activation volume,

$$V^* = \frac{d(\Delta H)}{d\sigma},$$

calculated from Eq. [6], is

$$V^* = baL. \quad [7]$$

For the parameters measured by microscopy, this value becomes 7.5×10^{-25} m^3, also well above the experimentally estimated apparent V^* of 1.2×10^{-26} m^3.

While the parameters calculated have much higher values than have ever been observed in doped tungsten, or other dispersion strengthened materials, the particular models assumed in obtaining these theoretical values may be in error without invalidating the general concept. For instance, both Guyot and Coulomb assume that the entire dislocation line between the obstacles is activated, and that it retains a circular shape during activation. This requirement seems unnecessary, and postulation of activation of only a portion of the dislocation line near the obstacle might lead to much lower activation energies and volumes.

SUMMARY AND CONCLUSIONS

The creep and rupture properties of 218 type doped tungsten wire were measured as a function of stress, temperature, and grain aspect ratio. Agreement with earlier work was obtained in observing that strength, and dependence of strength (rupture time or creep rate) on temperature and stress could be extremely high. The importance of grain morphology was demonstrated by showing that a critical grain aspect ratio was required for the attainment of maximum creep resistance. This critical gar was approximately 11 in this material, and clearly defined two different regimes of deformation. The low gar regime was strongly sensitive to grain aspect ratio and showed creep characteristics associated with grain boundary sliding and cavitation. In the high gar regime, however, creep was independent of grain aspect ratio, and appeared to be controlled by a dispersion strengthening of the crystal by dislocation–dope bubble interaction. Estimation of the extent of strengthening to be expected from the measured characteristics of the dispersion were in good agreement with the actual strength increment of doped over undoped material. This suggested that creep in doped tungsten is controlled by a thermally activated movement of a dislocation loop past the bubbles, but the exact nature of the bypass event is not known.

ACKNOWLEDGMENTS

The author is indebted to E. Koch and J. Walter of General Electric Corporate Research and Development for performing the foil making and microscopy of these wires, and to D. B. Snow of General Electric Refractory Metals Laboratory for additional microscopy and helpful discussions of this work. D. White of Refractory Metals Laboratory kindly supplied the undoped zone recrystallized tungsten for testing.

REFERENCES

1. D. B. Snow: *Met. Trans. A,* 1976, vol. 7A, pp. 783-94.
2. H. Warlimont, G. Necker, and H. Schultz: *Z. Metallkund.,* 1975, vol. 66, pp. 279-86.
3. D. M. Moon and R. C. Koo: *Met. Trans.,* 1971, vol. 2, pp. 2115-22.
4. O. Horascek: *Z. Metallkund.,* 1972, vol. 63, pp. 269-73.
5. D. M. Moon and R. Stickler: *High Temp.–High Pressure,* 1971, vol. 3, pp. 503-16.
6. J. W. Pugh: *Met. Trans.,* 1973, vol. 4, pp. 533-38.
7. B. A. Wilcox and A. H. Clauer: *Acta Met.,* 1972, vol. 20, pp. 743-57.
8. J. S. Benjamin and M. J. Bomford: *Met. Trans.,* 1974, vol. 5, pp. 615-21.
9. O. Horascek: *Z. Metallkund.,* 1974, vol. 65, pp. 318-23.
10. E. F. Koch and J. L. Walter: *Trans. TMS-AIME,* 1968, vol. 242, pp. 157-60.
11. C. R. Barrett and O. D. Sherby: *Trans. ASM,* 1966, vol. 59, pp. 3-15.
12. F. Garofalo, L. Zwell, A. S. Keh, and S. Weissmann: *Acta Met.,* 1961, vol. 9, pp. 721-29.
13. J. vanLanduyt, R. Gevers, and S. Amelinckx: *Phys. Status Solidi,* 1965, vol. 10, pp. 319-35.
14. R. Lagneborg: *Int. Metallogr. Rev.,* 1972, vol. 17, pp. 130-46.
15. P. L. Threadgill and B. Wilshire: *Metal Sci.,* 1974, vol. 8, pp. 117-24.
16. C. W. Corti, P. Cotterill, and G. A. Fitzpatrick: *Int. Metallogr. Rev.,* 1974, vol. 19, pp. 77-88.
17. S. L. Robinson and O. D. Sherby: *Acta Met.,* 1969, vol. 17, pp. 109-25.
18. J. J. Petrovic and L. J. Ebert: *Met. Trans.,* 1973, vol. 4, pp. 1301-08.
19. G. S. Ansell and J. Weertman: *Trans. TMS-AIME,* 1959, vol. 215, pp. 838-43.
20. P. Guyot: *Acta Met.,* 1962, vol. 12, pp. 665-67.
21. M. S. Grewal, S. A. Sastri, and N. J. Grant: *Met. Trans. A,* 1975, vol. 6A, pp. 1393-1404.
22. R. W. Weeks, S. R. Pati, M. F. Ashby, and P. Barrand: *Acta Met.,* 1969, vol. 17, pp. 1403-10.
23. I. Berlec: *Met. Trans.,* 1970, vol. 1, pp. 2677-83.
24. E. W. Hodkin, M. G. Nicholas, and D. M. Poole: *J. Less-Common Metals,* 1970, vol. 20, pp. 93-103.
25. M. H. Richman: *Trans. ASM,* 1967, vol. 60, p. 719.
26. M. F. Ashby: *Oxide Dispersion Strengthening,* 2nd Bolton Landing Conference, 1966, pp. 143-205, Gordon and Breach, N.Y., 1968.
27. L. M. Brown and R. K. Ham: *Strengthening Methods in Crystals,* pp. 9-135, Wiley, N.Y., 1971.
28. P. Coulomb: *Acta Met.,* 1959, vol. 7, pp. 556-59.
29. P. Guyot: *Acta Met.,* 1964, vol. 12, pp. 941-45.